

PreGSU: A Generalized Traffic Scene Understanding Model for Autonomous Driving based on Pre-trained Graph Attention Network

Yuning Wang, Zhiyuan Liu, Haotian Lin, Junkai Jiang, Shaobing Xu*, Jianqiang Wang*

Abstract—Scene understanding, defined as learning, extraction, and representation of interactions among traffic elements, is one of the critical challenges toward high-level autonomous driving (AD). Current scene understanding methods mainly focus on one concrete single task, such as trajectory prediction and risk level evaluation. Although they perform well on specific metrics, the generalization ability is insufficient to adapt to the real traffic complexity and downstream demand diversity. In this study, we propose PreGSU, a generalized pre-trained scene understanding model based on graph attention network to learn the universal interaction and reasoning of traffic scenes to support various downstream tasks. After the feature engineering and sub-graph module, all elements are embedded as nodes to form a dynamic weighted graph. Then, four graph attention layers are applied to learn the relationships among agents and lanes. In the pre-train phase, the understanding model is trained on two self-supervised tasks: Virtual Interaction Force (VIF) modeling and Masked Road Modeling (MRM). Based on the artificial potential field theory, VIF modeling enables PreGSU to capture the agent-to-agent interactions while MRM extracts agent-to-road connections. In the fine-tuning process, the pre-trained parameters are loaded to derive detailed understanding outputs. We conduct validation experiments on two downstream tasks, i.e., trajectory prediction in urban scenario, and intention recognition in highway scenario, to verify the generalized ability and understanding ability. Results show that compared with the baselines, PreGSU achieves better accuracy on both tasks, indicating the potential to be generalized to various scenes and targets. Ablation study shows the effectiveness of pre-train task design.

Index Terms—Autonomous Driving, scene understanding, interaction learning, pre-train mechanism, graph attention network.

I. INTRODUCTION

Autonomous Driving (AD) has made great progress in recent years and is expected to significantly improve traffic efficiency and safety. Measured by the automation-level defined by SAE, many industrial manufacturers have proposed L2+ AD applications, realizing partially automated functions in regular traffic scenes. However, the ability of current systems to cope with complicated interactive scenarios still needs to be proved [1]. Towards high-level AD there are still difficulties.

Scene understanding, defined as the learning, extraction and representation of the interactions in traffic scenarios through

raw perception information, is one of the critical challenges for high-level AD [2, 3]. The AD technology framework can be divided into perception, scene understanding, decision-making, and control [4]. Scene understanding involves risk assessment, trajectory prediction, intention recognition, etc. [5], and its role is to reason the inner relationships among the vehicles, road, and other traffic elements so that the decision-making module could have sufficient restrictions and goals to generate appropriate behaviors [6]. With the breakthrough of deep learning (DL) method in recent years, some end-to-end models that directly output control quantities with raw perception inputs were proposed; most methods integrate the scene understanding as encoders or feature engineering modules into the over DL network [7]. In summary, whether for hierarchical or end-to-end architecture, scene understanding is an inevitable procedure.

Current scene understanding methods can roughly divided into two categories, i.e., rule-based models and the data-driven ones. Li et al. surveyed the scene risk assessment metrics and concluded that in specific traffic scenarios, pre-defined models such as time-to-collision and time headway could express the interactions [8]. On the other hand, thanks to the emergence of large-scale AD datasets, DL models are capable of learning interactions among the agents, roadmap, and drivers [9]. Su et al. proposed a surrounding-aware LSTM model to predict the vehicle’s behavior in highway car-following cases [10]. Li et al. utilized deep reinforcement learning based on transformers to make lane change strategies [11]. Although these approaches have achieved good performance in specific situations, two main challenges hinder them in high-level AD applications. First, current scene understanding modules lack generalization ability and are only designed for limited tasks and traffic conditions [5]. Second, focusing on detailed downstream tasks such as trajectory prediction or risk level judgment results in overfitting to non-common scenario features. For instance, a model trained by car-following dataset cannot fully understand the interactions in crowded urban scenes, causing improper outputs [12]. In summary, it’s hard to strike a balance between performance and generalization ability.

This work is supported by the National Natural Science Foundation of China under Grant 52131021 (the key project), 52372415, and 52221005. This work is also supported by Tsinghua University Toyota Joint Research Center for AI Technology of Automated Vehicle (TTRS 2023-06) (*Corresponding author: Shaobing Xu, Jianqiang Wang.*)

Yuning Wang, Junkai Jiang, Shaobing Xu, and Jianqiang Wang are with School of Vehicle and Mobility, Tsinghua University, Beijing 100084, China. Zhiyuan Liu and Haotian Lin are with Xingjian College, Tsinghua University, Beijing 100084, China.

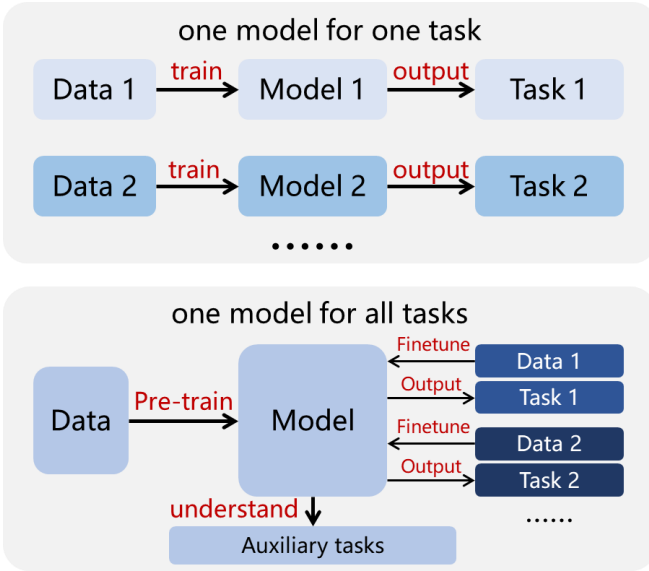


Fig. 1. Comparison of two scene understanding modes

Fig. 1 demonstrates two different scene understanding modes. As summarized above, the current pattern is that one network solves one task. In this mode, the total model size is large since parameters among various tasks cannot be generalized and reused, and for each new task, an entire training process is required which is time-consuming. Instead of focusing on specific downstream tasks, a better pattern is to design one unified model for all tasks. As illustrated in Fig. 1, a general model first learns the basic and interaction representation by pre-training on auxiliary tasks, then conducts small-scale finetuning to finish understanding tasks. Compared with the task-driven mode, this pattern shares a common backbone model, reducing the total parameter size. In addition, the finetuning process only requires relatively small-scale data and fewer epochs for training, making the time and data demands of developing a new understanding task fewer. Based on the above analysis, this study aims to build a universal medium layer for scene understanding, ensuring the adaptation of various succession downstream task modules.

In recent research, graph-based DL methods have been proven to be a good medium form to reflect the traffic scene understanding, extracting the spatiotemporal dependencies [13, 14]. By encoding agents, lanes, and other elements into subgraph nodes and interaction features into edges, a scene can be represented by an interpretable style while also transitive by neural networks, as shown in Fig. 2. In this study, we adopt the dynamic weighted graph as the data structure and graph attention network as the model backbone structure. Apart from the data structure and model backbone, training procedure also plays a vital role in the model performance. Pre-train mechanism has been proven to be useful in enhancing the model performance and interpretability in DL applications such as natural language processing and perception [15], which inspires traffic scene understanding. In this research, in contrast with training on the final task directly, we utilize pre-train into the traffic understanding model to increase the understanding performance and model generalization ability.

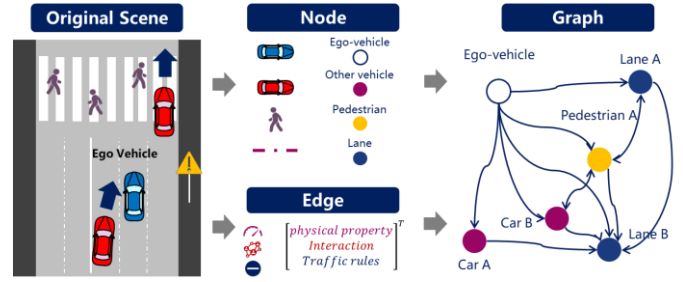


Fig. 2. An illustration of representing scene by graph

In this paper, we propose PreGSU, a novel pre-trained graph scene understanding model based on graph attention network for learning spatial-temporal interactions in traffic scenarios, acting as a universal medium layer for various downstream evaluation tasks. A self-supervised graph attention network is constructed based on the two designed pre-train tasks: masked roadmap modeling (MRM) and virtual interaction force (VIF) modeling. The MRM task captures the agent-to-lane relationship, while the novel-designed VIF modeling task based on driving safety field theory offers agent-to-agent reasoning. To illustrate the generalization ability of the proposed model, we validate the performance of PreGSU on two different downstream tasks: multi-modal trajectory prediction in urban scenarios and intention recognition in highway scenarios. The main contributions of this study are summarized below:

- 1) We present a novel universal medium module PreGSU based on pre-trained graph attention network for generalized traffic scene understanding.
- 2) Based on the analysis of traffic interaction mechanisms of various driving elements, we design two corresponding pre-train tasks to learn the interactions among agents and roadmap.
- 3) Experiments on two different downstream tasks demonstrate that PreGSU can realize precise scene understanding, proving the generalization ability.

The rest of this article is organized as follows: Section II summarizes the related works about scene understanding methods involving the rule-based and DL-based categories. Section III introduces the detailed structure of PreGSU, including the overall pre-train framework, feature engineering, backbone network design, pre-train task design, and training procedures. Experiments and analysis on pre-train and downstream tasks are conducted in Section IV. Section V gives the conclusions and future works.

II. RELATED WORKS

A. Rule-based scene understanding models

Rule-based scene understanding can be divided into four categories. The first category measures the interactions by simple metrics based on physical properties such as TTC, THW, etc. [16]. Based on physical properties, some studies use Gaussian distribution to consider the uncertainty in situation awareness [17, 18]. Although these metrics are lucid and explainable while easy to compute, they cannot cope with complicated scenarios where risk exists on multiple dimensions.

The second class utilized a finite state machine that switches among predefined modes and sets the corresponding understanding outputs. Bahram et al. proposed an interaction-aware prediction by discretizing the surrounding situations into various types and selecting the suitable method to make predictions [19]. Ulbrich et al. used embedded state machines in the Markov process to assess the decision-making under lane-changing scenarios [20]. While the performance is good in specific scenarios, such as a fixed intersection, it cannot deal with uncertain new scenes because of the prerequisites for defining state machines manually, leading to poor generalization performance.

The third category establishes the interaction system based on the game theory, giving the actions among the participants of a traffic scene rewards or punishments. Bahram et al. proposed a cooperative-driving prediction and planning framework based on dynamic game theory [21]. Li et al. further defined the game theoretic modeling among the driver and the vehicles toward autonomous vehicle control [22]. This category also demands manual discretized classification of driver's behaviors, and the computation cost grows exponentially when more participants engage.

Artificial potential field is also a widely used rule-based method for scene understanding. Transferring events into individual sources that generate energy, scenario interaction intensity can be expressed by a quantitative and continuous energy field distribution. Hang et al. used field energy as the risk assessment medium tool to make behavior decisions [23]. Wang et al. proposed Driving Safety Field consisting of three types of various field models [24]. Although field-based methods can effectively reflect the interaction of the scenario, they require complex traverse computation on a densely rasterized grid map, which makes the real-time efficiency not suitable for on-road applications.

Based on the above review, rule-based scene understanding methods are limited by strong rule constraints, resulting in low generalization ability. And some of them demand complex computation, failing to meet the real-time efficiency demand. However, some of the rule-based methods can effectively reason the interactions in the scenarios, serving as important references for offline modules that do not require real-time efficiency such as the design of pre-training tasks.

B. Deep learning scene understanding models

Due to the size explosion of autonomous driving datasets in the past few years, a lot of deep learning scene understanding models have emerged.

Since scene understanding is not an abstract concept, most studies focus on trajectory prediction, which possesses explicit evaluation metrics. In the early stage, sequential models such as Recurrent Neural Network (GRU) and Long-short Term Memory (LSTM). Park et al. proposed an LSTM-based encoder to analyze the fundamental patterns in past trajectories and an LSTM-based decoder to generate future trajectory sequences [25]. Other than sequential models, Dynamic Bayesian Network is also applied to contain more vehicle dynamics [26, 27]. Since the attention layer was proposed [28], attention-

based models including Transformer have become the mainstream backbone model for trajectory prediction, proving to be more effective. Chen et al. utilized non-autoregressive transformer based on a multi-head attention layer to predict highway scenarios [29]. Tian et al. applied masked autoencoder mechanism on transformer network to conduct trajectory prediction in urban cases [30]. Although the prediction accuracy is greatly improved through these methods, the connection to autonomous applications is limited due to a lack of generalization ability.

Some studies break the limitations of single tasks and explore the more macroscopic and generalized task of traffic scene understanding, and the graph-based DL model is a good representation form [31]. Hu et al. proposed UniAD, an integrated framework for scene understanding and planning based on attention mechanism [32]. Yang et al. proposed a scene understanding module based on a convolutional neural network to measure the importance of the regions [33]. Yu et al. designed a scene-graph data-driven risk assessment method for AD [14]. Monninger et al. established a traffic scene reasoning module based on a graph attention network to model the masked node properties [34]. Though they have extracted scene understanding as an individual module, most studies still validated the performance on a single task. In this work, we aim at design a unified scene understanding method to support various downstream tasks, reducing the transfer learning cost for AD applications.

Pre-train mechanism has been proven to enhance generalization ability and understanding performance in natural language processing and computer vision fields [35, 36]. By first training on simple but general tasks, the model backbone parameters can learn a universal understanding so that with few-shot fine-tuning process, it can support various specific downstream tasks. In this study, we refer to the pre-train structure and build a scene-understanding model for autonomous driving.

III. METHODS

A. Framework

The framework of the proposed PreGSU is shown in Fig. 3. The input information consists of a semantic roadmap and the agent history features. In the feature engineering procedure, lanes are expressed by polyline segments to maintain the same input dimension of agent data. Considering the perception error in the dataset, we only consider the lanes and agents within a fixed range, and for those outside the range, a mask is given. Then to express the vectorized data into the graph structure, the subgraph encoder, which is composed of Multi-Layer Perceptron (MLP), is applied to transfer the lanes and agents into nodes. Subsequently, the nodes are organized into the global graph and extract the interactions among them by multiple self-attention layers and cross-attention layers. Then the scene understanding module is trained on two self-supervised pre-train tasks: Virtual Interaction Force (VIF)

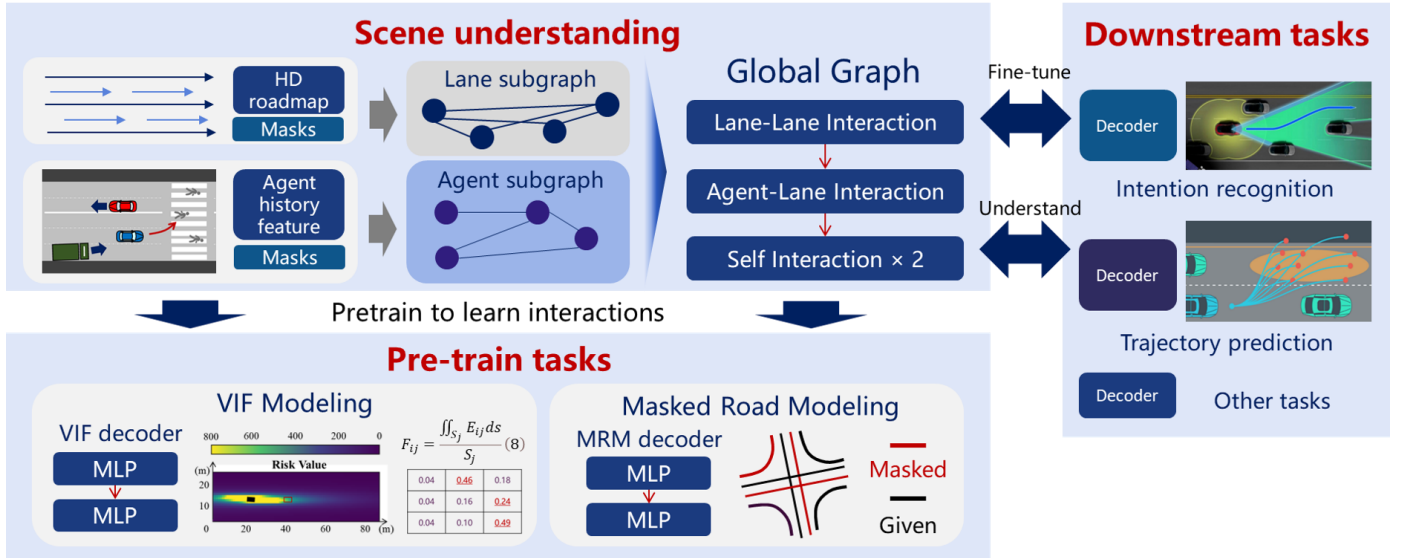


Fig. 3. The framework of PreGSU

modeling and Masked Road Modeling (MRM). Through epochs of pre-train, VIF enables PreGSU to reason the agent-to-agent interactions, and MRM enables the model to learn the interactions among the agents and lanes. After the pre-train procedure, PreGSU has learned the interaction beneath scenarios and has been able to support various kinds of concrete downstream tasks. In this study, we take intention recognition and multi-modal trajectory prediction as two examples of downstream applications of PreGSU, using the performance of these detailed tasks to verify the generalization and understanding ability. For each task, a decoder based on small-scale MLP is utilized to adjust the output format and dimension. Details of PreGSU are shown in the following sections.

B. Feature Engineering

From the raw data of complex traffic scene, we first extract useful features and organize them into a fixed format for model input. Specifically, a piece of traffic scene data usually includes information about the trajectories of agents and information about road topology. Following the vectorized representation [37], we organize the trajectories and road topology into polylines.

1) Agents

The trajectory of an agent can be represented by a sequence of states with position, velocity, and attribute information at each timestep. Specifically, the feature vector of an agent i at timestep t can be represented as (1) and (2):

$$A_t^i = [\mathbf{start}_t^i, \mathbf{end}_t^i, \mathbf{v}_t^i, \mathbf{a}^i] \quad (1)$$

$$\mathbf{v}_t^i = [v_x, v_y] \quad (2)$$

where $\mathbf{start}_t^i, \mathbf{end}_t^i$ are the coordinates of the start and end points of the agent motion vector at timestep t , \mathbf{v}_t^i is the velocity vector containing the velocity in the x and y direction, and \mathbf{a}^i is the attribute of agent i (i.e., vehicle, pedestrian, cyclist, etc.). The final feature vector A^i of agent i is the concatenate of A_t^i along time t , resulting in the shape of $T \times d_a$, where T is the

total timesteps of agents' trajectories and d_a is the feature dimension. To be noted that since we have got serial agent position coordinates, the heading angles information have been implicitly included and can be inferred by network.

Following the agent-centric representation, we set the origin of the coordinates at the target agent's current position $\mathbf{x}_0 \in \mathbf{R}^2$ and the positive direction of x -axis on the current heading θ_0 . Given a coordinate \mathbf{x} of raw data, this transformation can be expressed by (3) and (4):

$$\mathbf{x}' = (\mathbf{x} - \mathbf{x}_0) * \mathbf{R} \quad (3)$$

$$\mathbf{R} = \begin{bmatrix} \cos\theta_0 & -\sin\theta_0 \\ -\sin\theta_0 & \cos\theta_0 \end{bmatrix} \quad (4)$$

where \mathbf{R} is the rotation matrix according to θ_0 .

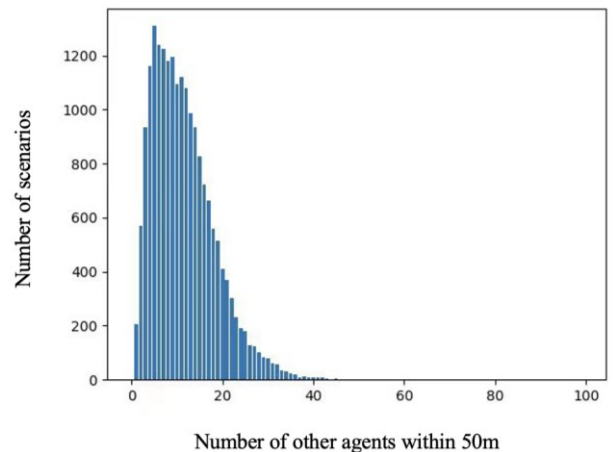


Fig. 4. Distribution of the number of other agents within 50m

One problem for agent feature engineering is that the number of agents could be very large in some scenarios, while only few of them have enough impact on the target agent. Some studies show that considering too many agents may lead to poorer results [38], since the impact of those distant agents on the ego

vehicle is subtle. As shown in Fig. 4, most scenarios contain fewer than 20 other agents within 50m. Therefore, we simply filter them by the relative distance to the target agent. Specifically, we sort the relative distance, and the $N_a = 20$ nearest agents are retained. Zero-padding is applied for scenarios that contain fewer than N_a agents. Therefore, all the scenarios will have agent features $A \in \mathbf{R}^{N_a \times T \times d_a}$.

2) Roadmap

In semantic HD maps, each lane can be represented as a sequence of vectors to approximate its basic geometry. Specifically, the feature vector of the part j of lane i can be represented as (5):

$$M_j^i = [\mathbf{start}_j^i, \mathbf{end}_j^i, \mathbf{a}^i] \quad (5)$$

where \mathbf{start}_j^i and \mathbf{end}_j^i are the coordinates of the start and end points, and \mathbf{a}^i is the binary attribute vector of lane i , e.g., whether this segment has a turn direction or controlled by a traffic light. The final feature vector M^i of lane i is the concatenate of M_j^i along the dimension j , resulting in the shape of $L \times d_m$, where L is the total number of vectors of a lane, and d_m is the feature dimension.

Similarly, the map features are transformed into the agent-centric coordinate frame. We apply the same filter strategy as agents, where N_m nearest lanes are retained, formulating the map feature $M \in \mathbf{R}^{N_m \times L \times d_a}$.

C. Model Architecture

As shown in Fig. 3, our scene understanding model consists of two parts: Subgraph Encoder and global graph encoder based on Heterogeneous Attention layers. Subgraph encoder aggregates the history information of each agent and the geometry information of each lane. Then global graph further models the interactions between them. The output of the scene understanding model is a generalized scene representation and can be utilized by different subsequent decoders to achieve variable tasks, such as trajectory prediction and intention recognition.

1) Subgraph encoder

Given agent feature input $A \in \mathbf{R}^{N_a \times T \times d_a}$ and map feature input $M \in \mathbf{R}^{N_m \times L \times d_a}$, the subgraph decoder aggregates the information along dimension T for agent features and dimension L for map features, to obtain polyline-level features $A_s \in \mathbf{R}^{N_a \times D}$ and $M_s \in \mathbf{R}^{N_m \times D}$ for subsequent interaction modeling, where D is the feature dimension.

Our subgraph encoder is a three-layer PointNet-like polyline encoder [39], as shown in (6):

$$(P_j^i)^{(l+1)} = \text{MLP}([\text{MLP}((P_j^i)^{(l)}), \varphi(\text{MLP}((P_j^i)^{(l)}))] \quad (6)$$

where P_j^i is the j^{th} segment of polyline i , which can be A_t^i or M_j^i , MLP is a multilayer perceptron network, φ is a max-pooling operator, l represents the l^{th} layer of the subgraph encoder, and P^i denotes all the segments of this polyline. For

each layer of the subgraph encoder, the features of each segment are encoded by MLP and interact with each other by concatenating and max pooling. Another MLP is applied for further fusion of each segment. Finally, a max-pooling operation is used to obtain the polyline-level feature, which is conducted by (7).

$$P_s = \varphi((P^i)^{(3)}) \quad (7)$$

2) Global graph encoder

For each agent, the future behavior is related to the historical state, other agents' behavior, and the road topology. The first item is modeled by subgraph encoder, and the last two still need to be further encoded. Specifically, we use a graph attention network [40] to model the interactions between heterogeneous input, i.e., maps and agents. Instead of processing all the tokens in the attention layer, we apply the hierarchical structure, which first handles agent interactions as well as map-agent interactions, followed by all token interactions to further encode interaction information, as shown in Fig. 5. This structure benefits from the hierarchical design, reducing the time complexity from $O((N_a + N_m)^2)$ to $O(N_a^2 + N_m^2)$.

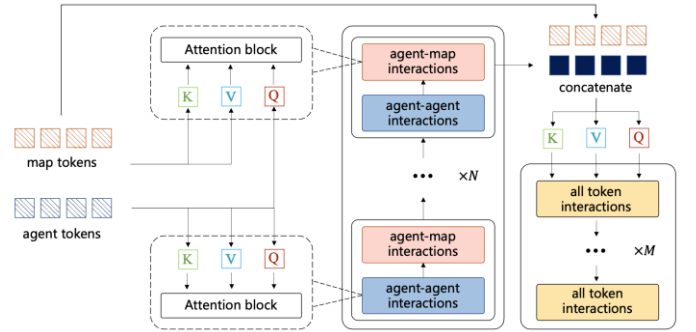


Fig. 5. Hierarchical attention structure of global graph encoder

For agent interactions, we use the output of the subgraph encoder A_s to formulate query, key, and value, as shown in (8) and (9):

$$Q = W_q A_s, \quad K = W_k A_s, \quad V = W_v A_s \quad (8)$$

$$\widehat{A}_{s,a} = \text{softmax}\left(\frac{QK^T}{\sqrt{D}}\right)V \quad (9)$$

where $W_q, W_k, W_v \in \mathbf{R}^{D \times D}$ are linear layers and D is the feature dimension. Through the attention module, each pair of agents is given an attention score to model interactions between them, then the attention score is used to fuse features from different agent tokens. The result of the attention operation $\widehat{A}_{s,a}$ will be used to update A_s as shown in (10):

$$A_s = \text{MLP}(\widehat{A}_{s,a}) + A_s \quad (10)$$

where MLP is a multilayer perceptron network, A_s on the right side of the equation is the value before the update and represents

the residual connection [41].

For agent-map interactions, we use the output of the subgraph encoder A_s as query and M_s as key and value, as demonstrated in (11) and (12):

$$Q = W_q A_s, \quad K = W_k M_s, \quad V = W_v M_s \quad (11)$$

$$\widehat{A_{s,m}} = \text{softmax}\left(\frac{QK^T}{\sqrt{D}}\right)V \quad (12)$$

Similar to agent interactions, the attention module calculates the attention intensity between each agent-map pair, representing the allocation of attention to different lanes by each agent, and then fuses information from these lanes. $\widehat{A_{s,m}}$ will be used to update A_s in the same way as described in (10).

The agent interaction and agent-map interaction are repeated N times alternately. After this operation, the updated A_s aggregates preliminary information about agent interactions and road topology. To further fuse the information of all tokens, we introduce the all-token interactions. In this module, $C = [A_s, M_s] \in \mathbf{R}^{(N_a + N_m) \times D}$ is used as query, key, and value. Similar to the modules above, the all-token interactions can be calculated as (13), (14), and (15):

$$Q = W_q C, \quad K = W_k C, \quad V = W_v C \quad (13)$$

$$\widehat{C} = \text{softmax}\left(\frac{QK^T}{\sqrt{D}}\right)V \quad (14)$$

$$C = \text{MLP}(\widehat{C}) + C \quad (15)$$

All-token interactions are repeated M times, in which all tokens can attend to each other freely to facilitate further feature fusion. Through the designed graph attention network, each token fuses sufficient interaction tokens with other tokens and contains high-level information on agent interactions and road topology, thus can be further used by different downstream decoders.

D. Pre-train task design

The model architecture designed allows the network parameters to have sufficient potential and a reasonable mechanism to learn the ability of scene understanding. Meanwhile, pre-train tasks guide the direction of parameter evolution, which is equally crucial for scene understanding.

In this study, to encompass general and comprehensive features, we start from the mechanism analysis of scenario interaction to design the pre-train tasks. As shown in Fig. 6, analyzing the interaction mechanism, two main factors influence the behavior of the ego vehicle: roadmap restriction and agent restriction [5]. Studies have proven that roadmap topology greatly restricts the vehicle's future motion [42]. Due to the roadmap constraints, the vehicles can only drive along the lanes, enabling that all possible vehicle behaviors quickly converges to a limited number of modalities. Since, under most situations, although few intensive agent-to-agent interactions

occur, only considering roadmap restriction is sufficient to achieve a good understanding. On the other hand, agent restriction is another crucial factor in understanding the scenario [43]. Because of the agent's influence to each other, vehicles select an appropriate model to drive within the possible lane-restricted trajectories. In summary, in order for the model to adequately learn the scene interaction during the pre-train phase, it is necessary to design pre-train tasks containing roadmap restriction and agent restriction.

In this study, we design the Virtual Interaction Force (VIF) Modelling to learn agent-to-agent reasoning and Masked Roadmap Modelling (MRM) to learn agent-to-lane reasoning.

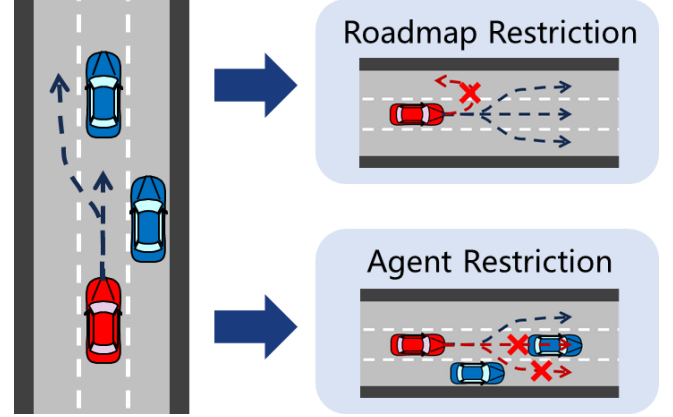


Fig. 6. An analysis of the vehicle interaction mechanism

1) Virtual Interaction Force modeling

Expressing the interaction among agents is complicated. Raw properties, including positions, velocities, etc., do not contain enough semantic information, while simple metrics such as time-to-collision and time headway only measure the interaction on specific single dimension. In recent years, field energy theory has been widely used because of its comprehensiveness. Each agent is considered a risk source that radiates energy, and the risk at a certain position in the scene is the sum of energy superimposed by multiple sources. Based on the field theory, Wang et al. proposed Driving Safety Field (DSF) which defined the modeling of the static potential field and dynamic kinetic field [24]. One problem is that computing the field requires multiple high-dimensional iterations on rasterized grid-based scenes thus the real-time performance is poor. For each frame, it takes approximately 0.2 seconds to calculate the field, making it difficult to implement on real-world understanding models. However, the pre-train process does not require real-time efficiency, and in this study, we develop the virtual force concept based on DSF to serve as the supervisory signal of the pre-train task aimed at extracting interactions among agents. According to the definition in [24], the static potential energy E_{static} at position (x, y) generated from an agent at position (x_a, y_a) is calculated as (16), where M_{eq} is the equivalent mass, r is the relative distance, v_a is the agent velocity, M is the vehicle mass, G , a , b , and c are constant coefficients. The dynamic kinetic energy is calculated as (17) to (19), where $\Delta \mathbf{v}$ is the relative velocity vector, \mathbf{v} is the

velocity vector of the target agent, \mathbf{v}_a is the velocity vector of the agent, $\Delta \mathbf{r}$ is the relative position vector, k_1 and k_2 are constant coefficients. Then the overall risk energy is computed as (20).

$$E_a^{static} = \frac{GM_{eq}}{r^2} = \frac{GM(a \cdot v_a^c + b)}{(x_a - x)^2 + (y_a - y)^2} \quad (16)$$

$$E_a^{dynamic} = k_1(\Delta \mathbf{v})^2 \frac{e^{k_2(\Delta \mathbf{v} \cdot \Delta \mathbf{r})}}{r} \quad (17)$$

$$\Delta \mathbf{v} = \mathbf{v} - \mathbf{v}_a \quad (18)$$

$$\Delta \mathbf{r} = (x - x_a, y - y_a) \quad (19)$$

$$E_a = E_a^{static} + E_a^{dynamic} \quad (20)$$

Based on the field energy, we further apply the VIF concept to transfer the two-dimension field map into an interaction vector. As demonstrated in Fig. 7, considering the area covered by the ego vehicle's bounding box, the virtual force can be decoupled into the components from various risk sources. The force generated from Agent i denoted as F_i is defined as the average energy intensity in the bounding box area S , as shown in (21).

$$F_i = \frac{\iint_S E_i ds}{S} \quad (21)$$

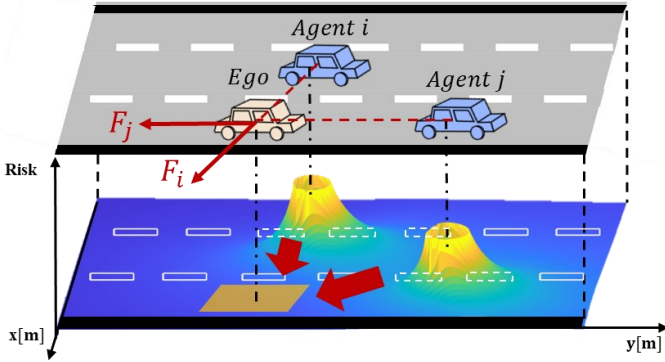


Fig. 7. An illustration of Virtual Interaction Force concept

After computing the forces other agents impose on the ego vehicle, normalization in (22) is conducted to show the comparative interaction intensity since, in real traffic, what really matters is the relative influences. Then, organize the forces into the VIF vector as (23), where N_a is the agent number considered in our model as introduced in previous sections. During the pre-train phase, the training target is to fit the **VIF** vector for each case with the input of history into information.

$$\bar{F}_i = \frac{F_i - \min_{j \in A} F_j}{\max_{j \in A} F_j - \min_{j \in A} F_j} \quad (22)$$

$$\mathbf{VIF} = [\bar{F}_1 \quad \dots \quad \bar{F}_{N_a}] \quad (23)$$

2) Masked Roadmap Modeling

As for the MRM pre-training task, we refer to the design in [42]. The semantic roadmap is a graph topology consisting of polyline segments. Each lane segment is connected and neighbored by others, so we can infer the position and shape of a lane through the information about its surroundings. As shown in Fig. 8, the dotted lines represent masked lanes that need to be modeled, and the solid lines denote the known ones.

For each case, the masks are randomly distributed. As for the masking ratio, we refer to the ablation study results in [42] and set to 50%.

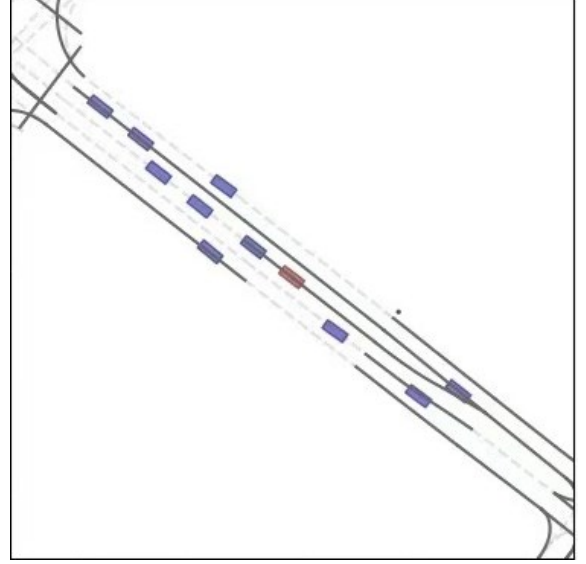


Fig. 8. An illustration of Masked Roadmap Modelling pre-training task

IV. IMPLEMENTATION AND EXPERIMENTS

In this study, we select two downstream tasks to validate the scene understanding performance, which are the multi-modal trajectory prediction in an urban environment and the intention recognition in highway environment. Diversity in the understanding of target and scenario conditions can also validate the generalization ability.

The overall procedure of application on specific task is: pre-training on VIF modeling and MRM, loading the pre-train parameters, and fine-tuning on the tasks.

A. Pre-train implementation

As introduced before, two pre-train tasks are utilized to make the inner parameters of PreGSU learn the spatial-temporal interactions beneath the scenes. One critical issue is how to design the loss function containing two tasks. As for the VIF modeling, we calculate \mathcal{L}_{VIF} as the mean squared errors of the ego vehicle's interaction forces to other agents, as shown in (24)

$$\mathcal{L}_{VIF} = \frac{\sum_{i \in A} (\bar{F}_i - \hat{F}_i)^2}{N_a} \quad (24)$$

where \bar{F}_i is the ground truth of VIF, \hat{F}_i is the predicted force of the ego vehicle to agent i , and A is the agent set considered, and

N_a is the agent number. To adjust the output format of PreGSU, a simple small-scale decoder is utilized, as shown in Fig. 9.

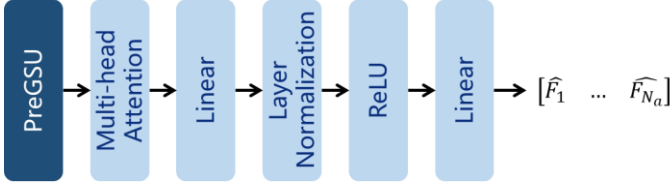


Fig. 9. The decoder for VIF modeling pre-train.

As for the masked lane modeling, we refer to the definition of forecast-MAE [42], using mean squared errors of L2 distance to calculate \mathcal{L}_{MRM} , as illustrated in (25)

$$\mathcal{L}_{MRM} = \frac{\sum_{i \in ML} \|\mathbf{start}^i - \widehat{\mathbf{start}}^i\| + \|\mathbf{end}^i - \widehat{\mathbf{end}}^i\|}{N_{ml}} \quad (25)$$

where \mathbf{start}^i and \mathbf{end}^i denote the ground truth of start and end points coordinates of lane segments, while $\widehat{\mathbf{start}}^i$ and $\widehat{\mathbf{end}}^i$ are the predicted coordinate vectors. Similar to VIF modelling, an MLP-based decoder is used to adjust the output dimensions, as illustrated in Fig. 10.

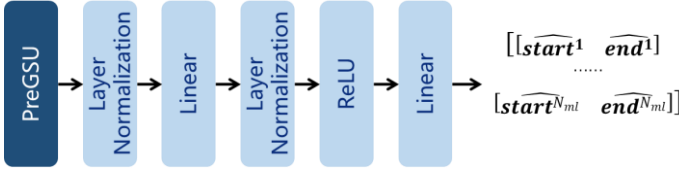


Fig. 10. The decoder for MRM pre-train.

The overall loss is the weighted sum of VIF error and MRM error, as shown in (26). The relative weights w_{VIF} and w_{MRM} are hyperparameters.

$$\mathcal{L}_{Pre} = w_{VIF} \mathcal{L}_{VIF} + w_{MRM} \mathcal{L}_{MRM} \quad (26)$$

Our models are implemented using *Pytorch lightning*. We used ADAM optimizer and a dynamic learning rate following the Cosine Annealing manner. The batch size is set to 64, the drop-out rate is set to 0.1, and the maximum training epoch is 60.

TABLE I
PRE-TRAIN RESULTS

$[w_{VIF}, w_{MRM}]$	\mathcal{L}_{VIF}	\mathcal{L}_{MRM}
[1, 1]	0.0179	0.0379
[5, 1]	0.0175	0.0369
[10, 1]	0.0175	0.0329
[40, 1]	0.0176	0.0381
[100, 1]	0.0178	0.0411

The training is conducted on a server with a NVIDIA A100 GPU. The pre-train results are shown in Table I. The best weights are selected as $w_{VIF} = 10$ and $w_{MRM} = 1$. The VIF loss reaches 0.0174, and the MRM loss reaches 0.0329. When

the weight is too small, the corresponding item cannot generate enough influence on the backward propagation. In contrast, if the weight is too large, the task overfits the data, which can decrease the understanding ability. Therefore, a ratio of 10:1 is the best weight setting, balancing the understanding ability of agents and roadmap interaction. Model parameters are saved as checkpoints, which can be loaded for the downstream tasks.

B. Multi-modal trajectory prediction in urban scenes

In the trajectory prediction task, we select the large-scale trajectory prediction dataset Argoverse-1 [44] to validate the scene understanding performance. The dataset provides the trajectory information and HD-map, and we extract the training and validation sets, which contain 205942 and 38742 samples, respectively. Each scenario is sampled at 10 Hz and consists of 2 seconds of history and 3 seconds of future. The trajectory prediction task is required to predict $K = 6$ future trajectories given the 2-second history and HD-map information.

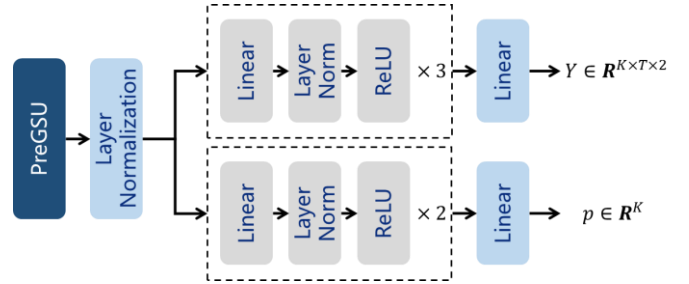


Fig. 11. The decoder for multi-modal trajectory prediction.

In this task, we use a four-layer MLP to predict the future trajectories $Y \in \mathbf{R}^{K \times T \times 2}$, and another three-layer MLP to predict the possibility $p \in \mathbf{R}^K$ of each trajectory, as shown in Fig. 11. The layers of agent interactions and agent-map interactions N is set to 2, and the layer of all-token interactions M is set to 3. We share the same training settings in the pre-train stage.

For the trajectory regression loss, we only calculate the SmoothL1 loss between the trajectory Y^{i^*} and the ground truth trajectory \hat{Y} with the smallest endpoint distance, as shown in (27) and (28):

$$L_{reg} = \text{SmoothL1}(Y^{i^*}, \hat{Y}) \quad (27)$$

$$\text{SmoothL1}(Y, \hat{Y}) = \frac{1}{n} \sum_{i=1}^n \begin{cases} 0.5(\hat{Y}_i - Y_i)^2 & |\hat{Y}_i - Y_i| < 1 \\ |\hat{Y}_i - Y_i| - 0.5 & |\hat{Y}_i - Y_i| \geq 1 \end{cases} \quad (28)$$

For the classification loss, we apply the Cross-Entropy loss to maximize the possibility p^{i^*} of Y^{i^*} , as shown in (29):

$$L_{cls} = - \sum_{i=1}^K \mathbb{I}(i = i^*) \log(p^i) \quad (29)$$

where \mathbb{I} is the binary indicator function. The final loss is the sum of the two losses.

Following the official evaluation metrics, we adopt minADE and minFDE to validate the performance. MinADE is the minimum time-average distance between the K predicted trajectories and the ground truth. MinFDE is the minimum end-point distance between the K predicted trajectories and the ground truth. The setting of optimizer, learning rate, and batch size is identical to the pre-train process.

We select LSTM, vanilla transformer, TNT [45], and GOHOME [46] as baselines for comparison, all of which are small-scale models with fewer than 1M parameters. The results of the Argoverse-1 validation set are shown in Table II. Our model outperforms all the baselines on the evaluation metrics, indicating good scene understanding ability. With 712k model parameters, our model achieves good performance compared with other small-scale trajectory prediction models of similar size.

TABLE II
MULTI-MODAL TRAJECTORY PREDICTION RESULTS

Methods	minADE	minFDE
LSTM	0.90	1.65
Vanilla Transformer	0.80	1.36
TNT	0.73	1.27
GOHOME	--	1.26
PreGSU	0.70	1.25

To further explore the role of pre-training for scene understanding, we conducted ablation experiments with different pre-training strategies, as shown in Table III. The pretrain mechanism decreases minFDE by 2.27% and minADE by 1.54%. Considering that the selected baselines are quite strong models specially designed for trajectory prediction, it is good for our method which aims at a more generalized usage to achieve such level of improvement. When only VIF is employed, the model performs even worse than the model without pretrain. A possible reason is that overemphasizing agent interaction may lead to active behavior changes, ignoring the roadmap restriction and making the trajectory similar to that under unstructured environments. When only MRM is applied, the performance is slightly better than the model without pre-train, proving that the MRM strategy helps to understand the road topology. When both strategies are applied, the model understands both agent interactions and road topology better, leading to the best performance in all metrics. In summary, our proposed pretrain strategy has the ability to allow the small-scale model to better understand the scene.

TABLE III
ABLATION EXPERIMENT OF TRAJECTORY PREDICTION RESULTS

Pre-train Configuration	minADE	minFDE
None	0.713	1.277
VIF	0.721	1.295
MRM	0.710	1.271
VIF+MRM	0.702	1.248

C. Intention recognition in highway scenes

In the intention recognition task, we select the HighD dataset to validate the scene understanding performance. HighD was collected in highway conditions from a bird-eye view, and the behaviors of vehicles can be classified into three kinds, which are driving straight, turning left, and turning right [47]. In the raw dataset, among the original about 11,000 vehicle trajectories, approximately 94.5% of the events are simple car-following. Such an imbalanced distribution will lead to meaningless high-accuracy metrics, failing to understand the high interaction cases. Therefore, we filtered and processed the dataset by retaining all over 6000 left-turn and right-turn trajectories while randomly selecting 6000 straight-driving ones to form a new training and validation set.

The intention recognition can be modeled as a classification problem. Denote I_a as the ground truth of an agent's intention, the output of the model is a predicted distribution $\widehat{p}(x)$ as shown in (30), where p_l , p_s , and p_r denote the possibility of left, straight, and right accordingly. Then, select the behavior with the highest possibility as the final predicted intention.

$$\widehat{p}(x) = [p_l \quad p_s \quad p_r] \quad (30)$$

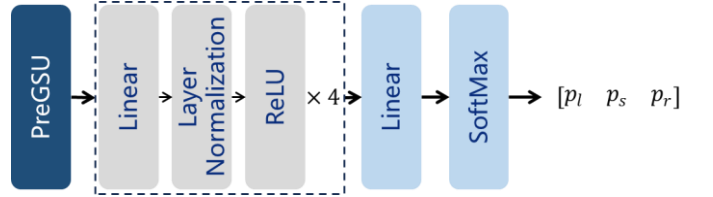


Fig. 12. The decoder for intention recognition.

The decoder used for PreGSU is a four-layer MLP followed by a SoftMax layer, as shown in Fig. 12. The validation metric is the recognition accuracy, while during the fine-tuning process, the training loss \mathcal{L}_{IR} selects cross entropy as shown in (31) where $p(x)$ is the ground truth binary distribution and $\widehat{p}(x)$ is the prediction intention distribution. The optimizer and learning rate setting is identical to the pre-train process. The batch size is set to 256.

$$\mathcal{L}_{IR} = - \sum_{x \in X} p(x) \log \widehat{p}(x) \quad (31)$$

We select GMM [48], LSTM [10], XYST [49], and DCIE [50] as the baselines for comparison, and the results of intention recognition accuracy are illustrated in Table IV. Our model outperforms all the baselines on the overall accuracy. Specifically, PreGSU exhibits a high accuracy of 98/26% in recognizing left-turn intention, proving a good understanding of interactive scenarios. The accuracy of straight-driving events is also the best. On the other hand, the right-turn accuracy is relatively low, and the possible reason is that sometimes the ground truth is not the most suitable driving according to the traffic rule, while through the pre-train process, the model tends to change to the left lane when both directions are equally drivable.

TABLE IV
INTENTION RECOGNITION ACCURACY RESULTS

Methods	Straight	Left	Right	Overall
GMM	87.10%	93.10%	92.40%	/
LSTM	93.10%	94.11%	88.80%	93.10%
XYST	90.88%	91.02%	92.05%	91.63%
DCIE	90.50%	94.80%	93.90%	93.07%
PreGSU	94.43%	98.26%	91.85%	95.11%

The ablation experiment results of the pre-train task design are illustrated in Tabel V. The pre-train mechanism increases the overall accuracy by 0.96%, and performances of all kinds of intention are improved. To be noted that, as for the intention recognition in highway scenarios, the agent interaction becomes more important since most lane-changing behaviors are caused by the hindrance of other vehicles. Therefore, different from the results of trajectory prediction, only applying the VIF modeling task also enhances the scene understanding ability.

TABLE V
ABLATION EXPERIMENT RESULTS OF INTENTION RECOGNITION

Pre-train Configuration	Straight	Left	Right	Overall
None	93.56%	97.33%	90.96%	94.15%
VIF	94.60%	97.63%	90.13%	94.39%
MRM	93.49%	97.80%	92.79%	94.93%
VIF+MRM	94.43%	98.26%	91.85%	95.11%

V. CONCLUSIONS AND FUTURE WORK

This paper proposed PreGSU, a pre-trained graph scene understanding model, to support various autonomous driving downstream tasks. The self-supervised graph attention network was established based on two designed pre-train tasks: masked roadmap modeling (MRM) and virtual interaction force (VIF) modeling. Experiments on two various downstream tasks, i.e., urban scene trajectory prediction and highway scene intention recognition, validated the scene understanding performance and generalization ability of PreGSU. The results indicated that the proposed model achieves the best performance compared with the baseline models on both tasks. In the urban trajectory prediction, the minADE and minFDE are 4.11% and 0.95% lower, while in the intention recognition task the overall accuracy is increased by 2.01%. In addition, ablation studies showed that the pre-train process improves the understanding performance. In summary, PreGSU has good ability to understand the spatial-temporal interactions in traffic scenes for autonomous driving.

In the future, we plan to explore the decision-making method based on the proposed scene understanding module and validate the performance on real-road tests. We also plan to analyze the transfer cost measured by data amount needed for fine-tuning among various downstream tasks to prepare for future real-traffic applications.

REFERENCES

- [1] X. Xu, L. Zuo, X. Li, L. Qian, J. Ren, and Z. Sun, "A reinforcement learning approach to autonomous decision making of intelligent vehicles on highways," *IEEE Transactions on Systems, Man, and Cybernetics: Systems*, vol. 50, no. 10, pp. 3884-3897, 2018.
- [2] K. K. Santhosh, D. P. Dogra, P. P. Roy, and B. B. Chaudhuri, "Trajectory-based scene understanding using Dirichlet process mixture model," *IEEE transactions on cybernetics*, vol. 51, no. 8, pp. 4148-4161, 2019.
- [3] L. Ye, Z. Wang, X. Chen, J. Wang, K. Wu, and K. Lu, "Gsan: Graph self-attention network for learning spatial-temporal interaction representation in autonomous driving," *IEEE Internet of Things Journal*, vol. 9, no. 12, pp. 9190-9204, 2021.
- [4] Z.-X. Xia *et al.*, "A Human-Like Traffic Scene Understanding System: A Survey," *IEEE Ind. Electron. Mag.*, vol. 15, no. 1, pp. 6-15, 2020.
- [5] Y. Wang *et al.*, "Decision-Making Driven by Driver Intelligence and Environment Reasoning for High-Level Autonomous Vehicles: A Survey," *IEEE Trans. Intell. Transp. Syst.*, pp. 1-20, 2023, doi: 10.1109/TITS.2023.3275792.
- [6] Y. Wang, J. Wang, J. Jiang, S. Xu, and J. Wang, "SA-LSTM: A Trajectory Prediction Model for Complex off-road Multi-agent Systems Considering Situation Awareness Based on Risk Field," *IEEE Trans. Veh. Technol.*, 2023.
- [7] Y. Huang and Y. Chen, "Autonomous driving with deep learning: A survey of state-of-art technologies," *arXiv preprint arXiv:2006.06091*, 2020.
- [8] Y. Li, Y. Zheng, B. Morys, S. Pan, J. Wang, and K. Li, "Threat assessment techniques in intelligent vehicles: A comparative survey," *IEEE Intell. Transp. Syst. Mag.*, vol. 13, no. 4, pp. 71-91, 2020.
- [9] Y. Wang, Z. Han, Y. Xing, S. Xu, and J. Wang, "A Survey on Datasets for the Decision Making of Autonomous Vehicles," *IEEE Intell. Transp. Syst. Mag.*, 2024.
- [10] S. Su, K. Muelling, J. Dolan, P. Palanisamy, and P. Mudalige, "Learning vehicle surrounding-aware lane-changing behavior from observed trajectories," in *Proc. 2018 IEEE Intelligent Vehicles Symposium (IV)*, 2018, pp. 1412-1417.
- [11] G. Li *et al.*, "Lane change strategies for autonomous vehicles: a deep reinforcement learning approach based on transformer," *IEEE Transactions on Intelligent Vehicles*, 2022.
- [12] D. Dauner, M. Hallgarten, A. Geiger, and K. Chitta, "Parting with Misconceptions about Learning-based Vehicle Motion Planning," *arXiv preprint arXiv:2306.07962*, 2023.
- [13] Y. Wang, Z. Liu, H. Lin, J. Li, R. Li, and J. Wang, "VIF-GNN: A Novel Agent Trajectory Prediction Model based on Virtual Interaction Force and GNN," in *Proc. 2023 IEEE Intelligent Vehicles Symposium (IV)*, 2023, pp. 1-7.
- [14] S.-Y. Yu, A. V. Malawade, D. Muthirayan, P. P. Khargonekar, and M. A. Al Faruque, "Scene-graph augmented data-driven risk assessment of autonomous vehicle decisions," *IEEE Trans. Intell. Transp. Syst.*, vol. 23, no. 7, pp. 7941-7951, 2021.
- [15] K. V. Alwala, A. Gupta, and S. Tulsiani, "Pre-train, self-train, distill: A simple recipe for supersizing 3d reconstruction," in *Proc. Proceedings of the IEEE/CVF Conference on Computer Vision and Pattern Recognition*, 2022, pp. 3773-3782.
- [16] J. Hillenbrand, A. M. Spieker, and K. Kroschel, "A multilevel collision mitigation approach—Its situation assessment, decision making, and performance tradeoffs," *IEEE Trans. Intell. Transp. Syst.*, vol. 7, no. 4, pp. 528-540, 2006.
- [17] H. Gao *et al.*, "Situational assessment for intelligent vehicles based on stochastic model and Gaussian distributions in typical traffic scenarios," *IEEE Transactions on Systems, Man, and Cybernetics: Systems*, vol. 52, no. 3, pp. 1426-1436, 2020.
- [18] M. Wang, L. Zhang, Z. Zhang, and Z. Wang, "An Enabling Decision-Making Scheme by Considering Trajectory Prediction and Motion Uncertainty," *IEEE Transactions on Intelligent Vehicles*, 2024.
- [19] M. Bahram, C. Hubmann, A. Lawitzky, M. Aeberhard, and D. Wollherr, "A combined model-and learning-based framework for interaction-aware maneuver prediction," *IEEE Trans. Intell. Transp. Syst.*, vol. 17, no. 6, pp. 1538-1550, 2016.
- [20] S. Ulbrich and M. Maurer, "Towards tactical lane change behavior planning for automated vehicles," in *Proc. 2015 IEEE 18th International Conference on Intelligent Transportation Systems*, 2015, pp. 989-995.
- [21] M. Bahram, A. Lawitzky, J. Friedrichs, M. Aeberhard, and D. Wollherr, "A game-theoretic approach to replanning-aware interactive scene

- prediction and planning," *IEEE Trans. Veh. Technol.*, vol. 65, no. 6, pp. 3981-3992, 2015.
- [22] N. Li, D. W. Oyler, M. Zhang, Y. Yildiz, I. Kolmanovsky, and A. R. Girard, "Game theoretic modeling of driver and vehicle interactions for verification and validation of autonomous vehicle control systems," *IEEE Transactions on control systems technology*, vol. 26, no. 5, pp. 1782-1797, 2017.
- [23] P. Hang, C. Lv, C. Huang, J. Cai, Z. Hu, and Y. Xing, "An integrated framework of decision making and motion planning for autonomous vehicles considering social behaviors," *IEEE Trans. Veh. Technol.*, vol. 69, no. 12, pp. 14458-14469, 2020.
- [24] J. Wang, J. Wu, and Y. Li, "The driving safety field based on driver-vehicle-road interactions," *IEEE Trans. Intell. Transp. Syst.*, vol. 16, no. 4, pp. 2203-2214, 2015.
- [25] S. H. Park, B. Kim, C. M. Kang, C. C. Chung, and J. W. Choi, "Sequence-to-sequence prediction of vehicle trajectory via LSTM encoder-decoder architecture," in *Proc. 2018 IEEE Intelligent Vehicles Symposium (IV)*, 2018, pp. 1672-1678.
- [26] X. Chen, H. Zhang, F. Zhao, Y. Cai, H. Wang, and Q. Ye, "Vehicle Trajectory Prediction Based on Intention-Aware Non-Autoregressive Transformer With Multi-Attention Learning for Internet of Vehicles," *IEEE Trans. Instrum. Meas.*, vol. 71, pp. 1-12, 2022.
- [27] Y. Jiang, B. Zhu, S. Yang, J. Zhao, and W. Deng, "Vehicle trajectory prediction considering driver uncertainty and vehicle dynamics based on dynamic bayesian network," *IEEE Transactions on Systems, Man, and Cybernetics: Systems*, vol. 53, no. 2, pp. 689-703, 2022.
- [28] A. Vaswani *et al.*, "Attention is all you need," in *Proc. Proceedings of the 31st International Conference on Neural Information Processing Systems*, 2017, pp. 6000-6010.
- [29] X. Chen, H. Zhang, F. Zhao, Y. Hu, C. Tan, and J. Yang, "Intention-aware vehicle trajectory prediction based on spatial-temporal dynamic attention network for Internet of Vehicles," *IEEE Trans. Intell. Transp. Syst.*, vol. 23, no. 10, pp. 19471-19483, 2022.
- [30] X. Tian, H. Ran, Y. Wang, and H. Zhao, "GeoMAE: Masked Geometric Target Prediction for Self-supervised Point Cloud Pre-Training," in *Proc. Proceedings of the IEEE/CVF Conference on Computer Vision and Pattern Recognition*, 2023, pp. 13570-13580.
- [31] S. Mylavarapu, M. Sandhu, P. Vijayan, K. M. Krishna, B. Ravindran, and A. Namboodiri, "Understanding dynamic scenes using graph convolution networks," in *Proc. 2020 IEEE/RSJ International Conference on Intelligent Robots and Systems (IROS)*, 2020, pp. 8279-8286.
- [32] Y. Hu *et al.*, "Planning-oriented autonomous driving," in *Proc. Proceedings of the IEEE/CVF Conference on Computer Vision and Pattern Recognition*, 2023, pp. 17853-17862.
- [33] S. Yang, W. Wang, C. Liu, and W. Deng, "Scene understanding in deep learning-based end-to-end controllers for autonomous vehicles," *IEEE Transactions on Systems, Man, and Cybernetics: Systems*, vol. 49, no. 1, pp. 53-63, 2018.
- [34] T. Moninger *et al.*, "Scene: Reasoning about traffic scenes using heterogeneous graph neural networks," *IEEE Robot. Autom. Lett.*, vol. 8, no. 3, pp. 1531-1538, 2023.
- [35] J. D. M.-W. C. Kenton and L. K. Toutanova, "BERT: Pre-training of Deep Bidirectional Transformers for Language Understanding," in *Proc. Proceedings of NAACL-HLT*, 2019, pp. 4171-4186.
- [36] T. Chen *et al.*, "The lottery tickets hypothesis for supervised and self-supervised pre-training in computer vision models," in *Proc. Proceedings of the IEEE/CVF conference on computer vision and pattern recognition*, 2021, pp. 16306-16316.
- [37] J. Gao *et al.*, "Vectormet: Encoding hd maps and agent dynamics from vectorized representation," in *Proc. Proceedings of the IEEE/CVF Conference on Computer Vision and Pattern Recognition*, 2020, pp. 11525-11533.
- [38] S. Shi, L. Jiang, D. Dai, and B. Schiele, "Mtr++: Multi-agent motion prediction with symmetric scene modeling and guided intention querying," *IEEE Transactions on Pattern Analysis and Machine Intelligence*, 2024.
- [39] C. R. Qi, H. Su, K. Mo, and L. J. Guibas, "Pointnet: Deep learning on point sets for 3d classification and segmentation," in *Proc. Proceedings of the IEEE conference on computer vision and pattern recognition*, 2017, pp. 652-660.
- [40] P. Veličković, G. Cucurull, A. Casanova, A. Romero, P. Liò, and Y. Bengio, "Graph Attention Networks," in *Proc. International Conference on Learning Representations*, 2018.
- [41] K. He, X. Zhang, S. Ren, and J. Sun, "Deep residual learning for image recognition," in *Proc. IEEE conference on computer vision and pattern recognition*, 2016, pp. 770-778.
- [42] J. Cheng, X. Mei, and M. Liu, "Forecast-mae: Self-supervised pre-training for motion forecasting with masked autoencoders," in *Proc. Proceedings of the IEEE/CVF International Conference on Computer Vision*, 2023, pp. 8679-8689.
- [43] Y. Wang, H. Huang, B. Zhang, and J. Wang, "A differentiated decision-making algorithm for automated vehicles based on pedestrian feature estimation," *IET Intelligent Transport Systems*, 2023.
- [44] M.-F. Chang *et al.*, "Argoverse: 3d tracking and forecasting with rich maps," in *Proc. IEEE/CVF conference on computer vision and pattern recognition*, 2019, pp. 8748-8757.
- [45] H. Zhao *et al.*, "Tnt: Target-driven trajectory prediction," in *Proc. Conference on Robot Learning*, 2021, pp. 895-904.
- [46] T. Gilles, S. Sabatini, D. Tsishkou, B. Stanciulescu, and F. Moutarde, "Gohome: Graph-oriented heatmap output for future motion estimation," in *Proc. 2022 international conference on robotics and automation (ICRA)*, 2022, pp. 9107-9114.
- [47] R. Krajewski, J. Bock, L. Kloeker, and L. Eckstein, "The highd dataset: A drone dataset of naturalistic vehicle trajectories on german highways for validation of highly automated driving systems," in *Proc. 2018 21st International Conference on Intelligent Transportation Systems (ITSC)*, 2018, pp. 2118-2125.
- [48] K. P. Murphy, *Dynamic bayesian networks: representation, inference and learning*. University of California, Berkeley, 2002.
- [49] Y. Zan, X. Wang, B. Xu, F. Feng, Z. Ling, and J. Song, "Lane Change Intention Recognition for Human Driving Vehicles under Moving Bottleneck on Freeway," in *Proc. 2022 IEEE 7th International Conference on Intelligent Transportation Engineering (ICITE)*, 2022, pp. 586-591.
- [50] B. Kim, C. M. Kang, J. Kim, S. H. Lee, C. C. Chung, and J. W. Choi, "Probabilistic vehicle trajectory prediction over occupancy grid map via recurrent neural network," in *Proc. 2017 IEEE 20th International Conference on Intelligent Transportation Systems (ITSC)*, 2017, pp. 399-404.



Yuning Wang received the bachelor's degree in automotive engineering from School of Vehicle and Mobility, Tsinghua University, Beijing, China, in 2020. He is currently pursuing the Ph.D. degree in mechanical engineering with School of Vehicle and Mobility, Tsinghua University, Beijing, China. His research centered on scene understanding, decision-making and planning, and driving evaluation of intelligent vehicles.



Zhiyuan Liu is a senior undergraduate student currently pursuing a bachelor's degree in Mechanics & Vehicle Engineering from Xingjian College, Tsinghua University, Beijing, China. His research interests include trajectory prediction and scene understanding of intelligent vehicles.



Haotian Lin is a senior undergraduate student from Xingjian College, Tsinghua University. His research concentrated on trajectory prediction and decision-making for autonomous vehicles. He is also interested in generative model control for autonomous driving applications.



Junkai Jiang received the bachelor's degree in automotive engineering from School of Vehicle and Mobility, Tsinghua University, Beijing, in 2021. He is currently pursuing the Ph.D. degree in mechanical engineering with School of Vehicle and Mobility, Tsinghua University, Beijing. His research interests include intelligent and connected vehicles, risk assessment, and decision making.



Shaobing Xu received his Ph.D. degree in Mechanical Engineering from Tsinghua University, Beijing, China, in 2016. He is currently an assistant professor with the School of Vehicle and Mobility at Tsinghua University, Beijing, China. He was an assistant research scientist and postdoctoral researcher with the Department of Mechanical Engineering and Mcity at the University of Michigan, Ann Arbor. His research focuses on vehicle motion control, decision making, and path planning for autonomous vehicles. He was a recipient of the outstanding Ph.D. dissertation award of Tsinghua University and the Best Paper Award of AVEC 2018 and 2022.



Jianqiang Wang received the B. Tech. and M.S. degrees from Jilin University of Technology, Changchun, China, in 1994 and 1997, respectively, and the Ph.D. degree from Jilin University, Changchun, in 2002. He is currently a Professor and the Dean of the School of Vehicle and Mobility, Tsinghua University, Beijing, China.

He has authored over 150 papers and is a co-inventor of over 140 patent applications. He was involved in over 10 sponsored projects. His active research interests include intelligent vehicles, driving assistance systems, and driver behavior. He was a recipient of the Best Paper Award in the 2014 IEEE Intelligent Vehicle Symposium, the Best Paper Award in the 14th ITS Asia Pacific Forum, the Best Paper Award in the 2017 IEEE Intelligent Vehicle Symposium, the Changjiang Scholar Program Professor in 2017, the Distinguished Young Scientists of NSF China in 2016, and the New Century Excellent Talents in 2008.